Journal Pre-proof

In vitro tripanocidal effect of 1,8-dioxooctahydroxanthenes (xanthenodiones) and tetraketones and improvement of cardiac parameters *in vivo*

Ana Paula de Jesus Menezes, Milene Lopes da Silva, Wagner Luiz Pereira, Guilherme de Paula Costa, Aline Luciano Horta, Andréa Aparecida Santos Mendonça, Ana Claudia Alvarenga Carneiro, Debora Maria Soares de Souza, Rômulo Novaes, Róbson Ricardo Teixeira, André Talvani

PII: S2213-7165(20)30097-7

DOI: https://doi.org/10.1016/j.jgar.2020.04.005

Reference: JGAR 1221

To appear in: *Journal of Global Antimicrobial Resistance*

Received Date: 28 January 2020

Revised Date: 2 April 2020

Accepted Date: 4 April 2020

Please cite this article as: Menezes APJ, Silva ML, Pereira WL, Costa GP, Horta AL, Mendonça AAS, Carneiro ACA, Souza DMS, Novaes R, Teixeira RR, Talvani A, *In vitro* tripanocidal effect of 1,8-dioxooctahydroxanthenes (xanthenodiones) and tetraketones and improvement of cardiac parameters *in vivo*, *Journal of Global Antimicrobial Resistance* (2020), doi: https://doi.org/10.1016/j.jgar.2020.04.005

Short title: Tripanocidal and inflammatory activities of xanthenodiones and tetraketones

In vitro tripanocidal effect of 1,8-dioxooctahydroxanthenes (xanthenodiones) and tetraketones and improvement of cardiac parameters *in vivo*

Ana Paula de Jesus Menezes[1], Milene Lopes da Silva[2], Wagner Luiz Pereira[2], Guilherme de Paula Costa[1], Aline Luciano Horta[1], Andréa Aparecida Santos Mendonça[3], Ana Claudia Alvarenga Carneiro[1], Debora Maria Soares de Souza[1], Rômulo Novaes[3], Róbson Ricardo Teixeira[2*], André Talvani[1*]

[1]Immunobiology Laboratory of Inflammation, Department of Biological Sciences, Universidade Federal de Ouro Preto, MG, Brazil; [2]Chemistry Department, Universidade Federal de Viçosa, MG, Brazil; [3]Department of Structural Biology, Universidade Federal de Alfenas, MG, Brazil.

***Corresponding authors:**

André Talvani

Laboratory of Immunobiology of Inflammation

DECBI/ICEB, Campus Morro do Cruzeiro

Universidade Federal de Ouro Preto, Ouro Preto, MG, Brazil

35400-000 Phone: 55 31 3559-1767 talvani@ufop.edu.br

Róbson Ricardo Teixeira

Departamento de Química

Universidade Federal de Viçosa, Viçosa, MG, Brazil

36570-900 Phone: 55 31 3612-6645 robsonr.teixeira@ufv.br

Abstract

Objetive. *Trypanosoma cruzi* infection affects millions of people worldwide, and the drugs available for its treatment have limited efficacy. 1,8-dioxooctahydroxanthenes and tetraketones are compounds with important biological applications. The aim of this study was to assess the trypanocidal and inflammatory activities of nine 1,8-dioxooctahydroxanthenes (**1**–**9**) and three tetraketones (**10**–**12**). **Methods and results.** By *in vitro* killing assay, three compounds were able to eliminate CL TdTomato expressing strain of *T. cruzi*, **9** (IC_{50} = 30.65 µM), **10** (IC_{50} = 14.11 µM), and **11** (IC_{50} = 26.43 µM). However, only **9** was not toxic to Vero cells. Next, to evaluate the *in vivo* antitrypanossomal and immunological efficacy of **9**, Swiss mice were infected with the Y and CL strains of *T. cruzi* and treated for 10 days with 50 mg/kg of **9**. This compound reduced the cardiac inflammatory infiltration in animals infected with both strains. RankL, CCL2, and IFN-γ were measured in the cardiac tissue homogenate of the Y-strain-infected animals, and no interference of **9** was observed. However, compound **9** increased the RankL and IL-10 levels in CL-infected mice. No hepatic and renal toxicity was observed. **Conclusion**. Our findings showed that 1,8-dioxooctahydroxanthene has anti-parasitic effect and ameliorates the cardiac inflammatory parameters related to *T. cruzi* infection.

Keywords: *Trypanosoma cruzi*; xanthenodiones; tetraketones, inflammation; heart damage; benznidazole.

1. Introduction

Trypanosoma cruzi is the causative agent of Chagas disease, and the World Health Organization estimates that approximately eight million people worldwide are infected with this parasite [1]. The infection in mammalian organisms induces intrinsic interactions between the parasite molecules and the host immune defense system. From this interaction, systemic and focal inflammatory responses are responsible for interrupting the parasitic replication [2-4]. Several investigations in experimental models of *T. cruzi* infection have suggested that a Th1-like immune response, mediated by T CD4+ and T CD8+ cells, is important for parasitism control through the production of pro-inflammatory cytokines (e.g., IFN, TNF, and IL-18), nitric oxide, and oxidative stress components [5-8]. Furthermore, during *T. cruzi* infection, IFN-γ also supports the activation of immune cells and the establishment of myocarditis by leukocyte recruitment through chemokines such as CCL5, CCL2, CXCL10, and CXCL9 [9, 10]. These chemokines are key proteins in the control of parasite replication as well as in the reinforcement of the induction of nitric oxide production by macrophages and infected cardiomyocytes [11]. Thus, therapeutic strategies that eliminate the parasites and ameliorate the tissue inflammatory response are of significant importance, especially considering the limited availability of drugs against *T. cruzi*. Currently, only the drugs nifurtimox and benznidazole are available. Benznidazole treatment presents questionable efficacy because of its mutagenic and carcinogenic activity [12].

The intensity of the inflammatory response during *T. cruzi* infection is related to distinct factors, such as the parasite strain, infection pathway, genetics, and immune response of the vertebrate host [13]. Therefore, the development of drugs that result not only in parasite elimination but also promote an equilibrium between the parasite and the host immune response is essential.

Within this context, several compounds have been evaluated for the treatment of American trypanosomiasis [14]. Described for the first time by Merlin (1894), tetraketone is an important class of compounds which is used as tyrosinase inhibitor [15], a laser dyes [16] and mainly as a lipoxygenase inhibitor and antioxidant agent [17]. The 1,8-dioxooctahydroxanthenes (also known as xanthenodiones) are heterocyclic compounds that possess a pyran nucleus fused on either side with cyclohex-2-enone rings. They present different biological activities including antibacterial [18], antifungal [19], antimalarial [20], leishmanicidal [21], and anti-inflammatory [22] effects. Considering that the laeishmanicidal and anti-inflammatory activities of xanthenodiones are closely related to *T. cruzi* pathogenesis, the aim of this study was to evaluate the trypanocidal action of 1,8-dioxooctahydroxanthenes and tetraketones *in vitro* and *in vivo*, and to verify their role in the reduction of levels of the parameters of inflammation in murine infection.

2. Material and methods

Synthesis

Generalities

All reagents were purchased from commercial sources (Sigma Aldrich; St. Louis, MO, USA and F Maia; Charqueada, São Paulo, Brazil) and were employed as received. Solvents were procured from F Maia and used as received. The ^{1}H (300 MHz) and ^{13}C nuclear magnetic resonance (NMR) (75 MHz) spectra were recorded on a Varian Mercury 300 instrument (Varian, Palo Alto, California, USA), using $CDCl_3$ and DMSO-d_6 as solvents. Hydrogen NMR data are presented as follows: chemical shift (δ) in ppm, number of hydrogen atoms, multiplicity, and J values in Hertz (Hz). Multiplicities are shown as the following abbreviations: s (singlet), d (doublet), m (multiplet), and t (triplet). Infrared spectra (IR) were obtained using the Agilent 660-IR (Santa Clara, California) with accessory GladiATR. Melting points are uncorrected and were determined using the MQAPF-301 melting point apparatus (Microquimica, Palhoça, Santa Catarina, Brazil). Mass spectra were obtained on a Shimadzu GCMS-QP5050A instrument (Kyoto, Japan) by direct injection using the following temperature program: 40 ^{o}C min^{-1} until the temperature reached 60 ^{o}C, and then 80 ^{o}C min^{-1} until the temperature reached 300 ^{o}C; the detector temperature was 280 ^{o}C. Analytical thin layer chromatography analyses were carried out on TLC plates recovered with 60GF254 silica gel.

*General procedure for the preparation of xanthenodiones **1-9***

A round-bottomed flask (25 mL) was charged with a 1,3-diketone (2.00 mmol), aldehyde (1.00 mmol), and $ZrOCl_2 \cdot 8H_2O$ (12.0 mg, 2 mol%). The mixture was stirred at 85 ^{o}C, and the progress of the reaction was monitored by TLC analysis. After completion of the reaction, the mixture was cooled down to 20 ^{o}C. Thereafter, 50 mL of dichloromethane was added, and the mixture was kept under stirring for

approximately 30 min. Then, the catalyst, which is insoluble in dichloromethane, was separated by filtration. After that, 50 mL of ethanol was added to the filtrate and the system was kept undisturbed for crystallization. The structures of xanthenodiones **1**-**9** (**Fig. 1**) are supported by the following data.

*9-(4-hydroxyphenyl)-3,4,5,6,7,9-hexahydro-1H-xanthene-1,8(2H)-dione (**1**)*

Brown solid (130.6 mg, 0.42 mmol, 42% yield). Mp 307 - 308 °C, IR (ATR) $\tilde{\nu}_{max}$/cm^{-1}: 3370, 2949, 2869, 1657, 1609, 1446, 1206, 1169 cm^{-1}. ^{1}H NMR (300 MHz, $CDCl_3$) δ: 9.16 (1H, s), 6.94 (2H, d, J = 8.4 Hz), 6.57 (2H, d, J = 8.4 Hz), 4.46 (1H, s), 2.69 – 2.51 (4H, m), 2.31 – 2.17 (4H, m), 1.99 – 1.76 (4H, m). ^{13}C NMR (75 MHz, $CDCl_3$) δ: 196.8, 164.9, 156.1, 135.5, 129.3, 116.4, 115.1, 36.9, 30.2, 26.9, 20.3. MS, *m/z* (%): 310 ($C_{19}H_{18}O_4$, M^+, 93), 293 (60), 253 (17), 217 (100), 55 (24).

*9-(3,4,5-trimethoxyphenyl)-3,4,5,6,7,9-hexahydro-1H-xanthene-1,8(2H)-dione (**2**)*

Yellow solid (358.8 mg, 0.93 mmol, 93% yield). Mp 188 - 189 °C. IR (ATR) $\tilde{\nu}_{max}$/cm^{-1}: 2963, 2882, 1659, 1619, 1453, 1230, 1170, 1123 cm^{-1}. ^{1}H NMR (300 MHz, $CDCl_3$) δ: 6.51 (2H, s), 4.77 (1H, s), 3.80 (6H, s), 3.75 (3H, s), 2.70 – 2.53 (4H, m), 2.44 – 2.27 (4H, m), 2.08 – 1.93 (4H, m). ^{13}C NMR (75 MHz, $CDCl_3$) δ: 196.6, 164.0, 152.8, 139.9, 136.7, 116.7, 105.7, 60.6, 56.6, 37.0, 31.4, 27.1, 20.3. MS, *m/z* (%): 384 ($C_{22}H_{24}O_6$, M^+, 60), 369 (13), 353 (100), 217 (27), 55 (12).

*9-(4-hydroxyphenyl)-3,6-dimethyl-3,4,5,6,7,9-hexahydro-1H-xanthene-1,8(2H)-dione (**3**)*

Yellow solid (87.4 mg, 0.26 mmol, 52% yield). Mp 215 - 216 °C. IR (ATR) $\tilde{\nu}_{max}$/cm^{-1}: 3600, 3274, 2998, 2964, 2876, 1658, 1638, 1609, 1188 cm^{-1}. ^{1}H NMR (300 MHz, DMSO) δ: 9.16 (1H, s), 6.92 (2H, d, J = 8.3 Hz), 6.56 (2H, d, J = 8.3 Hz), 4.45 and 4.43 (1H, s), 2.66 – 2.55 (2H, m), 2.50 – 2.21 (6H, m), 2.08 – 2.02 (2H, m), 1.01 – 0.91 (6H, m). ^{13}C NMR (75 MHz, DMSO) δ: 196.8, 196.7 and 196.6, 164.6, 164.5, 163.7 and 163.6, 156.1, 156.0, 135.5, 135.4, 135.2, 129.4, 129.3, 129.2, 116.1, 115.9, 115.7, 115.1, 115.0, 45.0, 44.9, 34.8, 34.3, 30.4, 30.2, 28.2, 28.1, 27.9, 20.8, 20.7. MS, *m/z* (%): 338 ($C_{21}H_{22}O_4$, M^+, 87), 321 (54), 268 (18), 245 (100), 203 (18), 69 (19).

*9-(4-hydroxyphenyl)-3,6-diisopropyl-3,4,5,6,7,9-hexahydro-1H-xanthene-1,8(2H)-dione (**4**)*

Yellow solid (22.7 mg, 0.58 mmol, 58% yield). Mp 176 - 177 °C. IR (ATR) $\tilde{\nu}_{max}$/cm^{-1}: 3405, 3172, 2959, 2873, 1671, 1645, 1612, 1463, 1372, 1181 cm^{-1}. ^{1}H NMR (300 MHz, DMSO-d_6) δ: 7.09 – 7.03 (2H, m), 6.61 – 6.55 (2H, m), 4.68 (1H, s), 2.66 – 2.32 (6H, m), 2.13 – 1.99 (2H, m), 1.96 – 1.79 (2H, m), 1.64 – 1.52 (2H, m), 0.94 - 0.89 (12H, m). ^{13}C NMR (75 MHz, DMSO) δ: 198.0, 197.7, 164.5, 164.4, 163.9, 154.8, 135.8, 135.6, 129.3, 116.8, 116.7, 116.4, 115.4, 41.4, 41.0, 40.1, 38.7, 31.8, 31.0, 30.8, 19.6, 19.5, 19.4. MS, *m/z* (%): 394 ($C_{25}H_{30}O_4$, M^+, 88), 377 (52), 351 (15), 301 (100), 296 (22), 41 (19).

*9-(3,4-dimethoxyphenyl)-3,3,6,6-tetramethyl-3,4,5,6,7,9-hexahydro-1H-xanthene-1,8(2H)-dione (**5**)*

Yellow solid (406.1 mg, 0.99 mmol, 99% yield). Mp 181 – 182 °C. IR (ATR) $\tilde{\nu}_{max}$/cm^{-1}: 2959, 2873, 1656, 1621, 1361, 1260, 1198, 1167, 1136 cm^{-1}. ^{1}H NMR (300 MHz, $CDCl_3$) δ: 6.89 (1H, s), 6.76 – 6.68 (2H, m), 4.68 (1H, s), 3.84 (3H, s), 3.78 (3H, s), 2.45 (4H, s), 2.23 (2H, d, J = 16.3 Hz), 2.16 (2H, d, J = 16.3 Hz), 1.09 (6H, s), 0.99 (6H, s). ^{13}C NMR (75 MHz, $CDCl_3$) δ: 196.5, 162.1, 148.4, 147.4, 136.9, 120.1, 115.7, 112.2, 110.8, 110.4, 55.8, 55.7, 50.7, 40.8, 32.2, 31.1, 29.3, 27.2. MS, *m/z* (%): 410 ($C_{25}H_{30}O_5$, M^+, 69), 379 (100), 273 (35), 217 (16), 83 (18).

*3,3,6,6-tetramethyl-9-(4-nitrophenyl)-3,4,5,6,7,9-hexahydro-1H-xanthene-1,8(2H)-dione (**6**)*

White solid (343.9 mg, 0.87 mmol, 87% yield). Mp 221 - 222 °C. IR (ATR) $\tilde{\nu}_{max}$/cm^{-1}: 2959, 2871, 1654, 1620, 1515, 1359, 1342, 1199, 1164, 1138 cm^{-1}. ^{1}H NMR (300 MHz, $CDCl_3$) δ: 8.08 (2H, d, J = 7.9 Hz), 7.46 (2H, d, J = 7.9 Hz), 4.81 (1H, s), 2.49 (4H, s), 2.24 (2H, d, J = 16.3 Hz), 2.15 (2H, d, J = 16.3 Hz), 1.10 (6H, s), 0.98 (6H, s). ^{13}C NMR (75 MHz, $CDCl_3$) δ: 196.3, 163.0, 151.5, 146.4, 129.3, 123.4, 114.5, 50.6, 40.8, 32.4, 32.2, 29.2, 27.2. MS, *m/z* (%): 395 ($C_{23}H_{26}NO_5$, M^+, 48), 378 (68), 348 (25), 273 (100), 217 (32), 161 (24), 152 (15), 77 (16), 55 (33), 43 (24), 41 (42).

*4-(3,3,6,6-tetramethyl-1,8-dioxo-2,3,4,5,6,7,8,9-octahydro-1H-xanthen-9-yl)benzonitrile (**7**)*

White solid (327.7 mg, 0.87 mmol, 87% yield). Mp 198 - 199 °C. IR (ATR) $\tilde{\nu}_{max}$/cm^{-1}: 2961, 2872, 2225, 1659, 1620, 1360, 1197, 1164, 1138 cm^{-1}. ^{1}H NMR (300 MHz, $CDCl_3$) δ: 7.50 (2H, d, J = 7.6 Hz), 7.40 (2H, d, J = 7.6 Hz), 4.75 (1H, s), 2.47 (4H, s), 2.23 (2H, d, J = 16.3 Hz), 2.14 (2H, d, J = 16.2 Hz), 1.10 (6H, s), 0.97 (6H, s). ^{13}C NMR (75 MHz, $CDCl_3$) δ: 196.3, 162.9, 149.5, 131.9, 129.3, 119.0, 114.5, 110.1, 50.6, 40.8, 32.5, 32.2, 29.2, 27.2. MS, *m/z* (%): 375 ($C_{24}H_{25}NO_3$, M^+, 41), 273 (100), 217 (21), 161 (14), 55 (22), 43 (17), 41 (33).

*3,3,6,6-tetramethyl-9-phenyl-3,4,5,6,7,9-hexahydro-1H-xanthene-1,8(2H)-dione (**8**)*

Yellow solid (275.7 mg, 0.79 mmol, 79% yield). Mp 203 - 204 °C. IR (ATR) $\tilde{\nu}_{max}$/cm^{-1}: 2957, 2871, 1659, 1624, 1359, 1197, 1164, 1139 cm^{-1}. ^{1}H NMR (300 MHz, $CDCl_3$) δ: 7.28 (2H, d, J = 7.5 Hz), 7.20 (2H, t, J = 7.5 Hz), 7.11 – 7.06 (1H, m), 4.74 (1H, s), 2.46 (4H, s), 2.23 (2H, d, J = 16.3 Hz), 2.15 (2H, d, J = 16.3 Hz), 1.09 (6H, s), 0.98 (6H, s). ^{13}C NMR (75 MHz, $CDCl_3$) δ: 196.4, 162.3, 144.1, 128.4, 128.0, 126.3, 115.6, 50.7, 40.9, 32.2, 31.8, 29.2, 27.3. MS, *m/z* (%): 350 ($C_{23}H_{26}O_3$, M^+, 49), 273 (100), 217 (23), 161 (8).

*9-(4-hydroxyphenyl)-3,3,6,6-tetramethyl-3,4,5,6,7,9-hexahydro-1H-xanthene-1,8(2H)-dione (**9**)*

White solid (355.5 mg, 0.91 mmol, 91% yield). Mp 250 - 251 °C. IR (ATR) $\tilde{\nu}_{max}$/cm^{-1}: 3401, 2961, 2872, 1660, 1613, 1358, 1199, 1165, 1133 cm^{-1}. ^{1}H NMR (300 MHz, $CDCl_3$) δ: 7.05 (2H, d, J = 8.1 Hz), 6.54 (2H, d, J = 8.1 Hz), 4.65 (1H, s), 2.45 (4H, s), 2.24 (2H, d, J = 16.5 Hz), 2.17 (2H, d, J = 16.5 Hz), 1.08 (6H, s), 0.99 (6H, s). ^{13}C NMR (75 MHz, $CDCl_3$) δ: 197.3, 162.5, 154.7, 135.5, 129.3, 115.8, 115.2, 50.7, 40.8, 32.3, 30.9, 29.3, 27.2. MS, *m/z* (%): 366 ($C_{23}H_{26}O_4$, M^+, 92), 349 (39), 282 (25), 273 (100), 217 (32), 161 (15), 83 (17).

*General procedure for the preparation of tetraketones **10-12***

The synthesis of compounds **10-12** (**Fig. 2**) has been previously described [23, 24]).

Biological Assays

Parasites and culture procedures in vitro

CL *T. cruzi* fluorescent parasites were generated by transfecting the parasite strain with pTREX-Td-tomato plasmid as described by Canavaci, Bustamante [25]. The CL DNA allows a good and efficient tagging by genetic manipulation and the transfection procedure and experimental conditions were previously reported by Peng and Tarleton [26]. The Vero cell monolayer cultures were infected with trypomastigote metacyclic forms of *T. cruzi*, and these cells were subsequently used in the amastigote growth inhibition assays. Infected Vero cells were cultured in RPMI 1640 medium with 10% fetal bovine serum in a humid atmosphere containing 5% CO_2 at 37°C.

Amastigote growth inhibition assay

Vero cells were exposed to 2000 rad of gamma radiation for 10 min [27]. Then, 2.5 × 10^4 cells were plated in 96-well plates (Black Greiner plates - Bio-One) overnight at 37 °C and under 5% CO_2. Vero cells were exposed to trypomastigotes of the CL tdTomato strain of *T. cruzi* for approximately 5 h at a multiplicity of infection ratio 1:10 cell/trypomastigotes. After infection, cell cultures were washed to remove non-internalized parasites. Then, fresh media with or without xanthenodiones (**1**-**9**), tetraketones (**10**-**12**), or benznidazole were added in decreasing concentrations (50µM/mL to 0.5 µM/mL). The change in fluorescence intensity was determined as a measurement of growth over 3 days of culture. The killing assays were performed by the average of the three independent experiments, in duplicate. The 50% inhibitory concentration (IC_{50}) and 50% cytotoxicity concentration (CC_{50}) values were determined by nonlinear regression analysis at day 3 using GraphPad Prism version 7. The selective index (SI) indicates the number of times the compounds were more toxic to the parasites than the mammalian cells, and it was calculated utilizing the CC_{50}/IC_{50} ratio.

Cell toxicity

To evaluate the toxic effect of compounds **1-12** on the mammalian cells, Vero cells were treated with decreasing concentrations of the compounds (100µM/mL to 1.5 µM/mL). The experiment was performed using Alamar Blue® (Bio-Rad, California, USA), a colorimetric index of cell proliferation, as described by Rampersad [28]. Vero cells were added (2.5×10^4 cells/well) on Black Greiner plates (Bio-One), and after cell adhesion, the compounds were diluted with DMSO (0.01%) in each well and maintained in a CO_2 incubator at 37 °C for 72 h. Each plate contained a negative control (medium) and a positive control (medium + cell). After 72 h of incubation, the culture medium was removed, and 10% Alamar Blue® reagent was added. After 4 h of incubation, the fluorescence was measured on the SynergyH4 plate reader (BioTek) at 560 and 590 nm wavelengths. The percentage of dye reduction induced by the compounds was calculated considering the percent reduction of incubated cells in the absence of compounds using the following equation:

$$\% \text{ reduction} = [A560-(A590 \times R0) \text{ Treated}/A560-(A590 \times R0) + \text{Control}]$$

In this equation, A560 = fluorescence at 560 nm; A590 = fluorescence at 590 nm; control = well containing cells, medium, and Alamar Blue in the absence of the compound; and R0 = the correction factor, calculated from the fluorescence emission values of the negative control (-C), only culture medium, and Alamar Blue® in the absence of cells [Ro = (A560/A590) C]. The results correspond to an average of three independent experiments in duplicate.

In vivo drug testing

Swiss female mice aged 4–6 weeks, were bred and maintained at the Center of Animal Science at the Federal University of Ouro Preto (UFOP), Brazil. The procedures adopted agreed with the ethical principles of animal experimentation pre-established by the National Council for Control of Animal Experimentation (CONCEA). This research was previously approved by the Ethics Committee on Animal Research of UFOP-CEUA (protocol nº 2016/34).

Parasites and infection

Swiss mice (n = 10) were infected intraperitoneally with 5×10^3 blood trypomastigote forms of *T. cruzi* strains CL and Y. Blood was stored in liquid nitrogen and maintained *in vivo* by successive passages in Swiss mice. The CL strain was isolated from a *Triatoma infestans* collected in Rio Grande do Sul, Encruzilhada, South Brazil, in 1963 [29]. For chemotherapy experiments, it presents a high susceptibility to drugs clinically used in Chagas disease [30] and it is classified as a discrete typing units (DTUs) VI [31]. The Y strain belongs to DTU II [31] and it was obtained from a female child patient in 1953 in São Paulo, Southeast Brazil [32]. Studies involving medical drugs against the *T. cruzi*, describes this strain as partially susceptible to Bz and it evolves intense inflammatory response in mammalian hosts [32]. For all this reason, both strains, CL and Y, might provide an adequate parasitological and inflammatory answers related to the test of new and potential compounds.

The parasitemia was determined daily by optic microscopy analysis of 5 µL samples, after tail bleeding [33].

Treatments and euthanasia

Treatments with xanthenodione **9** (50 mg/kg) and benznidazole (100 mg/kg) were initiated 4 days after infection with *T. cruzi* Y strain and 8 days after infection with the CL strain. After the establishment of *T. cruzi* infection, the compounds were administered for 10 consecutive days orally (gavage) at a volume of 0.2 mL of carboxymethylcellulose (CMC) 0.5% suspension plus Tween 80 (0.5% solution). The untreated animal received a vehicle content (CMC) 0.5% suspension plus Tween 80 (0.5% solution).

Animals (n = 10) were sorted into groups: (i) uninfected animals that received CMC + Tween 80; (ii) infected untreated mice that received CMC + Tween 80; (iii) infected mice treated with **9**; (iv) infected mice treated with benznidazole; and (v) uninfected mice treated with **9**. Animals in the acute phase were euthanized after 14 and 18 days for Y and CL strains, respectively, according to euthanasia practice guidelines regulated by the CONCEA. Blood and cardiac tissues were collected for biochemical tests, immunoassays, and histopathological analysis.

Evaluation of cytokines and chemokines by Immunoassays

Immunoenzymatic assays were used to evaluate the concentrations of the inflammatory cytokines IFN-gamma and RankL, the chemokine CCL2, and the regulatory cytokine IL-10. Cardiac tissues were isolated and macerated, and the supernatant was used according to the manufacturer's protocol (PeproTech Inc., Rocky Hill, NJ, USA). At the end of the reaction, 100 µL/well of the chromogen substrate ABTS (2,2′-azino-bis(3-ethylbenzothiazoline-6-sulfonic acid); Sigma-Aldrich Inc., St. Louis, MO, USA) was added for 60 min, followed by incubation in the dark at 25 ^{o}C. Finally, samples were read in a spectrophotometer (Emax Molecular Devices, Sunnyvale, CA, USA) using wavelengths of 405 and 630 nm.

Heart histopathology and stereology

Heart samples of all animals were fixed in 10% buffered formaldehyde for 48 h. The samples were embedded in glycol methacrylate histological resin and cut in a rotary microtome into 3-µm-thick sections using glass knives (Leica Biosystems, Wetzlar, Germany). Five histological sections were collected in semi-series, using one out of every 50 sections, which were stained with hematoxylin and eosin. Histopathological analysis was performed by evaluating the distribution and organization of the organ parenchyma and connective stroma, tissue necrosis and inflammatory infiltrate, morphology and distribution of myocytes, blood vessels, and interstitial cells, and the presence of *T. cruzi* amastigote nests [34].

The intensity of cellularity or heart inflammation was assessed by comparing the distribution of interstitial cells in the myocardium of all groups [35]. For this purpose, tissue cellularity per histological area was determined as the number of interstitial cell nuclei in a standardized test area (At = 25 × 10^3 μm^2). Tissue cellularity was evaluated from 20 randomly sampled histological fields of heart sections from each animal using a bright field microscope with a ×40 objective lens (400× magnification; Axioscope A1, Carl Zeiss, Germany). A total tissue area of 25.0 × 10^5 μm^2 was analyzed for each group. Total interstitial cellularity was analyzed using the image analysis software, Image-Pro Plus® (version 4.5; Media Cybernetics Inc., Silver Spring, MA, USA). The results are expressed as an octagonal field diagram organized in domains that represents tissue cellularity as follows: (-) minimum, (- - +) mild, (+ +) moderate or (+ + +) intense cellularity/inflammatory infiltrate [36].

The amplitude of the cardiac microstructural reorganization was analyzed using the stereological method [35]. Volume density (Vv, %) of heart parenchyma (cardiomyocytes [cmy]), stroma (connective tissue [cnt]), and blood vessels (bvs) were estimated as Vv= ΣPt/P, where ΣPt is the number of test points that hit on the structure of interest, and P is the total number of points in the test system. We used a test system with 72 test points in a standard test area (At = 25 × 10^3 μm^2) at the tissue level. The relationship between blood vessels and cardiomyocytes (Vv[bvs]/Vv[cmy]) was used as a morphological index of myocardium vascularization. The relationship between structural and functional heart compartments was estimated as Vv[cnt]/Vv[cmy]. Volume density was estimated from 20 randomly sampled histological fields of heart sections from each animal using a ×40 objective lens (400× magnification; Axioscope A1, Carl Zeiss, Germany). A total tissue area of 25.0 × 10^5 μm^2 was analyzed for each group.

The number density of mononuclear and polymorphonuclear interstitial cells per histological area was estimated as QA = ΣQ/At, where ΣQ is the number of mononuclear or polymorphonuclear in the microscopic focal plane, and At is the dimension of test area (At = 8.56×10^3 μm^2). Volume density was estimated from 20 randomly sampled histological fields of heart sections from each animal using a ×100 objective lens (1000× magnification; Axioscope A1, Carl Zeiss, Germany). A total tissue area of 85.6×10^4 μm^2 was analyzed for each group. All counts were performed using the image analysis software AxionVision (Carl Zeiss, Germany).

Hepatic and renal toxicity assays

Hepatic toxicity was assessed in order to detect the plasma levels of the enzymes aspartate aminotransferase and alanine aminotransferase. Urea and creatinine clearance were also detected in the plasma to identify renal damage. All the assays were performed using commercial enzymatic kits from Bioclin Labtest kits (Brazil).

Statistical analysis

The data obtained in the present investigation are expressed as the mean ± standard deviation. The GraphPad Prism v.6 (GraphPad Software, San Diego, CA, USA) program was used, and data were analyzed using the Kolmogorov-Smirnov test to confirm normality patterns. Depending on the nature of the data, one-way analysis of variance with post-test Bonferroni correction and the Kruskal-Wallis test with Tukey-Kramer and Dunn's post-tests were used for multiple comparisons. For all analyses, a significance level of $p \leq 0.05$ was adopted.

3. Results

Preparation of xanthenodiones and tetraketones

The xanthenodiones **1-9** herein investigated were synthesized via solvent-free zirconium-catalyzed Knoevenagel condensation between 1,3-diketones and appropriate aldehydes [23], as depicted in **Fig. 1**. The compounds were obtained with yields ranging from 42% to 99% and fully characterized via spectroscopic (infrared and nuclear magnetic resonance) and spectrometric (mass spectrometry) methods.

In addition to xanthenodiones, our research group has also been interested in the structural features (Silva *et al*., 2018) and biological activities of tetraketones. Thus, we undertook the task of evaluating the tripanocidal activity of the tetraketones **10-12** (**Fig. 2**).

To the best of our knowledge, this is the first time that xanthenodiones and tetraketones have been evaluated for their tripanocidal activity.

In vitro bioassays

Vero cells with and without infection with CLtdTomato parasites were treated or not treated with xanthenodiones **1-9**, tetraketones **10-12**, and benznidazole. The fluorescent intensity was measured on the third day of infection as an indicator of parasite growth. Among the twelve tested compounds, three showed anti-*T. cruzi* activities, namely, **9** (IC_{50} = 30.65 ± 1.0), **10** (IC_{50} = 14.11 ± 1.9), and **11** (IC_{50} = 26.43 ± 2.3) (**Fig. 3A & 3B**). However, tetraketones **10** and **11** showed high levels of toxicity to mammalian cells (**Fig. 3A** and **Table 1**).

Moreover, the xanthenodione **9** displayed a great SI (3.1) and no toxicity to Vero cells even at the highest tested concentration (**Table 1**). Therefore, compound **9** was selected to verify its capability of reducing the parasitemia and to alter the inflammatory parameters in *T. cruzi*-infected mice.

In vivo bioassays

Initially, we proceeded to determine a dose and route standardization for the treatment. Based on the number of surviving animals and parasitemia reduction, we selected an oral dosage of 50 mg/kg to start the experiment (data not shown). After 10 days of therapy using compound **9**, on the 14th and 18th days of infection with the Y and CL strains, respectively, we did not observe quantitative differences in the circulating levels of parasites in animals treated or untreated with **9**, the benznidazole treated group demonstrated a significant reduction (**Fig. 4A and B**). The treatment reduced the peak of parasitemia in the infected animals, which was responsible for a reduction in their mortality when compared to that in the untreated ones (**Fig. 4C and D**). Benznidazole treatment also prevented mice mortality for both tested strains.

By analyzing the levels of the inflammatory mediators on the myocardium, we observed an increase in RankL in animals infected with the CL strain and treated with **9** (**Fig. 5A**) and an increase of CCL2 (**Fig. 5B)** in the untreated animals when compared to uninfected mice. However, compound **9** was able to increase the plasma production of IFN-γ as well as IL-10 in the CL+**9** group (**Fig. 5C and D)**. Benznidazole administration was able to maintain the inflammatory mediators at basal levels close to the uninfected/treated and uninfected mice. A ratio of these inflammatory markers and the regulatory IL-10 is pointed out in **Table 2**.

Regarding the present investigation, the Y and CL strains of *T. cruzi* were associated with the prevalence of a moderate mononuclear cell influx, which was reduced upon treatment with **9** (**Fig. 6A & 6B**). The cardiac amastigote nests of the parasite were only observed in the infected and untreated mice (**Fig. 6C**). Furthermore, xanthenodione **9** treatment could reduce inflammatory infiltration for both

tested strains (**Fig. 6D**). In addition, cardiac damage caused by *T. cruzi* infection was prevented in groups treated with benznidazole, and no differences were observed between the uninfected and treated mice.

Compound **9** did not induce renal or liver toxicity. The levels of urea and creatinine did not increase in the plasma of any of the groups (**Table 3**). We verified an increase in aspartate aminotransferase and alanine aminotransferase levels in infected mice associated with the parasite infection (**Table 3**). In addition, there were no differences in the levels of markers between the uninfected and uninfected/treated mice, confirming the previous results.

4. Discussion

American trypanosomiasis still presents great impact in the population in tropical countries. The parasite-host interaction remains partially responsible for the absence of a therapeutic strategy against the *T. cruzi* [37]. In this sense, researchers have been struggling to find alternative compounds from different molecular scaffolds [38, 39]. It is outlined in **Fig. 7** the trials carried out in the present investigation.

From twelve compounds evaluated in this study, three presented trypanocidal activity. The technique used to generate xanthenodiones and tetraketones is called "green chemistry" since it is not harmful to the environment and environmentally acceptable [40, 41]. Low SI is a common problem faced by researchers who work with these compounds, mainly for the high cytotoxicity [42-44]. The same profile was also observed by Abe et al. (2004) who found unsatisfactory SIs, even when using *T. cruzi* strains Bz-susceptible. To reduce the harmful effects of xanthenodiones and tetraketones on mammalian cells and, consequently, to reduce their toxicity, authors have suggested small conformational changes in the molecule to guarantee the optimization of the compounds [45-47]. Although several potential molecules anti-*T. cruzi* are described annually, there is a failure in the *in vitro* and *in vivo* tests, which exclude the possibility of the compounds to move forward as efficient drugs [13]. Herein, we verified consistent results between the compounds activities in cellular and animal model. Our aim was not only to evaluate the anti-*T.cruzi* action, but also the action of the compounds on the inflammatory response. The choice of strains of the parasite was based on the protocols for the discovery of new drugs for Chagas disease [30]. In addition, the strains proposed in this assay allowed the rapid identification (less than 40 days) of an ideal dose required for subsequent steps in the screening process [38, 48-50]. In the animals infected with the Y strain of the *T. cruzi*, ten days of daily treatment were able to reduce the number of circulating parasites in fresh blood analysis in 40%, besides preventing the mortality of the animals. Parasitemia and mortality are basic criteria in the test of any new anti-*T. cruzi* compound [50]. For the CL strain, the pre-patent period occurs between the 6^{th} and 7^{th} days after infection and there is an increase in parasitemia from the 16^{th} day, reaching the peak on the 22nd day [51]. Our experiments were finished at the 18^{th} day post-infection, so that the same 10 days of treatment was maintained for both strains. Therefore, it was not possible to verify the parasitemia peak related to this strain.

During the acute infection driven by the *T. cruzi*, the exacerbated immune response is often observed systemically; in the myocardium, this results in lesions that, in extreme cases, can lead to death [52, 53]. Our results indicate the existence of a cardiac damage associated to the parasite strain and, although without parasitological cure, compound **9** proved to be effective in preventing cardiac injury in animals infected with both strains.

The trigger and the maintenance of the inflammatory response are directly related to the activation of cell signaling pathways, such as NF-kB [54-57]. In this context, we assessed the production of Rank's ligand (RankL), characterized as an activator receptor to the NF-kb pathway. There was no change in this inflammatory mediator in mice infected with the Y neither CL strain of *T. cruzi*, reinforcing the intrinsic strains features involved in the inflammatory context [30, 58-60].

Interestingly, the cardiac protection induced by **9** treatment in *T. cruzi*-infected mice (with Y and CL strains) was not followed by reduction of plasma levels of IFN-γ and CCL2. However, the balance between low IFN-γ and high IL-10 levels may represent a cardioprotective effect using different strains of the parasite [9, 11, 61-63], which could be a suggestive mechanism to explain our findings. Besides, the production of CCL2 is related to both parasitic growth and morphogenesis of trypomastigotes as well as increased activation and recruitment of inflammatory infiltration into the heart [62, 64, 65].

Finally, the treatment using compound **9** did not induce detectable adverse reactions in the mice. The increase in hepatic enzymes in the infected animals was possible caused by the metabolites generated from the *T. cruzi* infection [66]. Other studies shown that treatment with benznidazole was not able to raise the enzymes of liver damage, possibly for the short treatment period [67].

Thus, our *in vitro* findings showed that 1,8-dioxooctahydroxanthene (xanthenodione) has an anti-parasitic effect. In the acute murine infection, 10-days treatment with 50 mg/kg of xanthenodione **9** resulted in an inflammatory reduction associated to the *T. cruzi* infection. Notwithstanding, further investigations and new structural changes in the structure of **9** remain necessary to potentiate its trypanocidal and anti-inflammatory effects. However, in face to a scenario of failures in the field of anti-*T. cruzi* chemotherapy, the 1,8-dioxooctahydroxanthenes appear as new plastic and promising scaffold.

Acknowledgments

We thank our colleagues from Rick L. Tarleton's lab, University of Georgia, Athens/GA/EUA who provided insight and expertise that greatly assisted the *in vitro* research. AT (Process # 305634/2017-8) is grateful to the Conselho Nacional de Desenvolvimento Científico e Tecnológico (CNPq) for the research productivity fellowship.

Funding

This research was supported by CAPES, CNPQ, and FAPEMIG funding agencies in Brazil.

Competing Interests

None declared.

Ethical approval

This research was previously approved by the Ethics Committee on Animal Research of UFOP-CEUA (protocol nº 2016/34).

5. References

[1] WHO. World Health Organization - Chagas Disease. 2019.

[2] Rocha e Silva M. A brief survey of the history of inflammation. Agents and Actions. 1978;8:45-9.

[3] Marin-Neto JA, Cunha-Neto E, Maciel BC, Simoes MV. Pathogenesis of chronic Chagas heart disease. Circulation. 2007;115:1109-23.

[4] Talvani A, Teixeira MM. Chapter 8 - Inflammation and Chagas Disease: Some Mechanisms and Relevance. In: Weiss LM, Tanowitz HB, editors. Advances in Parasitology: Academic Press; 2011. p. 171-94.

[5] Padilla AM, Bustamante JM, Tarleton RL. CD8+ T cells in *Trypanosoma cruzi* infection. Current opinion in immunology. 2009;21:385-90.

[6] Coelho PS, Klein A, Talvani A, Coutinho SF, Takeuchi O, Akira S, et al. Glycosylphosphatidylinositol-anchored mucin-like glycoproteins isolated from *Trypanosoma cruzi* trypomastigotes induce in vivo leukocyte recruitment dependent on MCP-1 production by IFN-γ-primed-macrophages. 2002;71:837-44.

[7] Machado FS, Souto JT, Rossi MA, Esper L, Tanowitz HB, Aliberti J, et al. Nitric oxide synthase-2 modulates chemokine production by *Trypanosoma cruzi* infected cardiac myocytes. Microbes and infection. 2008;10:1558-66.

[8] Vespa GN, Cunha FQ, Silva JS. Nitric oxide is involved in control of *Trypanosoma cruzi* induced parasitemia and directly kills the parasite in vitro. Infection and immunity. 1994;62:5177-82.

[9] Machado FS, Dutra WO, Esper L, Gollob KJ, Teixeira MM, Factor SM, et al. Current understanding of immunity to *Trypanosoma cruzi* infection and pathogenesis of Chagas disease. Seminars in immunopathology. 2012;34:753-70.

[10] Talvani A, Ribeiro CS, Aliberti JCS, Michailowsky V, Santos PVA, Murta SMF, et al. Kinetics of cytokine gene expression in experimental chagasic cardiomyopathy: tissue parasitism and endogenous IFN-γ as important determinants of chemokine mRNA expression during infection with *Trypanosoma cruzi*. Microbes and Infection. 2000;2:851-66.

[11] Machado Fabiana S, Martins Gislâine A, Aliberti Júlio CS, Mestriner Fabiola LAC, Cunha Fernando Q, Silva João S. Trypanosoma cruzi infected cardiomyocytes produce chemokines and cytokines that trigger potent nitric oxide–dependent trypanocidal activity. Circulation. 2000;102:3003-8.

[12] Caldas IS, Talvani A, Caldas S, Carneiro CM, de Lana M, da Matta Guedes PM, et al. Benznidazole therapy during acute phase of Chagas disease reduces parasite load but does not prevent chronic cardiac lesions. Parasitol Res. 2008;103:413-21.

[13] Chatelain E. Chagas Disease Drug Discovery:Toward a New Era. 2015;20:22-35.

[14] Scarim CB, Jornada DH, Chelucci RC, de Almeida L, dos Santos JL, Chung MC. Current advances in drug discovery for Chagas disease. European Journal of Medicinal Chemistry. 2018;155:824-38.

[15] Khan KM, Maharvi GM, Khan MT, Jabbar Shaikh A, Perveen S, Begum S, et al. Tetraketones: a new class of tyrosinase inhibitors. Bioorg Med Chem. 2006;14:344-51.

[16] Zhongjiao Ren WC, Weiqi Tong & Xiuping Jing. Knoevenagel condensation of aldehydes with cyclic active methylene compounds in water. Synthetic Communications. 2002;32:13:1947-52.

[17] Maharvi GM, Ali S, Riaz N, Afza N, Malik A, Ashraf M, et al. Mild and efficient synthesis of new tetraketones as lipoxygenase inhibitors and antioxidants. J Enzyme Inhib Med Chem. 2008;23:62-9.

[18] Narasimha Murthy YL, Mahesh P, Devi BR, Durgeswarai LK, Mani P. Synthesis and Antibacterial Assay of 9-Substituted Aryl-1,8-dioxo-octahydroxanthenes. Asian Journal of Chemistry. 2014;26:4594-8.

[19] Rahimifard M, Mohammadi Ziarani G, Badiei A, Asadi S, Abolhasani Soorki A. One-pot solvent-free synthesis of 1,8-dioxo-octahydroxanthene derivatives using sulfonic acid-functionalized LUS-1 and their antimicrobial activities. Research on Chemical Intermediates. 2015;42:3847-61.

[20] Winter RW, Ignatushchenko M, Ogundahunsi OA, Cornell KA, Oduola AM, Hinrichs DJ, et al. Potentiation of an antimalarial oxidant drug. Antimicrob Agents Chemother. 1997;41:1449-54.

[21] Muhammad Nisar IA, Muhammad Raza Shah, Amir Badshah, Mughal Qayum, Humayun Khan, Inamullah Khand and Sajid Alia Amberlite IR-120H as a recyclable catalyst for the synthesis of 1,8-dioxo-octahydroxanthene analogs and their evaluation as potential leishmanicidal agents. RSC Advances. 2013;3.

[22] Cidade H, Rocha V, Palmeira A, Marques C, Tiritan ME, Ferreira H, et al. In silico and in vitro antioxidant and cytotoxicity evaluation of oxygenated xanthone derivatives. Arabian Journal of Chemistry. 2017.

[23] da Silva ML, Teixeira RR, de Azevedo Santos L, Martins FT, Ramalho TC. Synthesis and special characterization through X-ray analysis of 1,8-dioxooctahydroxanthenes. Arabian Journal of Chemistry. 2017.

[24] da Silva ML, Teixeira RR, de Azevedo Santos L, Martins FT, Ramalho TC. Structural analysis of two tetraketones and theoretical investigation of the reactions involved in their preparation. Journal of Molecular Structure. 2018;1156:700-11.

[25] Canavaci AM, Bustamante JM, Padilla AM, Perez Brandan CM, Simpson LJ, Xu D, et al. In vitro and in vivo high-throughput assays for the testing of anti-*Trypanosoma cruzi* compounds. PLoS Negl Trop Dis. 2010;4:e740.

[26] Peng D, Tarleton R. EuPaGDT: a web tool tailored to design CRISPR guide RNAs for eukaryotic pathogens. Microb Genom. 2015;1:e000033.

[27] Yan W, Moreno SN. A method to assess invasion and intracellular replication of *Trypanosoma cruzi* based on differential uracil incorporation. J Immunol Methods. 1998;220:123-8.

[28] Rampersad SN. Multiple applications of Alamar Blue as an indicator of metabolic function and cellular health in cell viability bioassays. Sensors (Basel). 2012;12:12347-60.

[29] Brener Z, Chiari E. The effects of some immunosuppressive agents in experimental chronic Chagas's disease. Trans R Soc Trop Med Hyg. 1971;65:629-36.

[30] Filardi LS, Brener Z. Susceptibility and natural resistance of *Trypanosoma cruzi* strains to drugs used clinically in Chagas disease. Transactions of the Royal Society of Tropical Medicine and Hygiene. 1987;81:755-9.

[31] Zingales B, Andrade S, Briones M, Campbell D, Chiari E, Fernandes O, et al. A new consensus for *Trypanosoma cruzi* intraspecific nomenclature: second revision meeting recommends TcI to TcVI %J Memórias do Instituto Oswaldo Cruz. 2009;104:1051-4.

[32] Amato Neto V. Origin of the "Y strain" of *Trypanosoma cruzi*. J Revista do Instituto de Medicina Tropical de São Paulo. 2010;52:171-.

[33] Brener Z. Therapeutic Activity and Criterion of Cure on Mice experimentally infected with *Trypanosoma cruzi*. Revista do Instituto de Medicina Tropical de Sao Paulo. 1962;4:389-96.

[34] Novaes RD, Sartini MV, Rodrigues JP, Goncalves RV, Santos EC, Souza RL, et al. Curcumin Enhances the Anti-Trypanosoma cruzi Activity of Benznidazole-Based Chemotherapy in Acute Experimental Chagas Disease. Antimicrob Agents Chemother. 2016;60:3355-64.

[35] Novaes RD, Penitente AR, Goncalves RV, Talvani A, Peluzio MC, Neves CA, et al. Trypanosoma cruzi infection induces morphological reorganization of the myocardium parenchyma and stroma, and modifies the mechanical properties of atrial and ventricular cardiomyocytes in rats. Cardiovasc Pathol. 2013;22:270-9.

[36] Felizardo AA, Caldas IS, Mendonca AAS, Goncalves RV, Tana FL, Almeida LA, et al. Impact of Trypanosoma cruzi infection on nitric oxide synthase and arginase expression and activity in young and elderly mice. Free Radic Biol Med. 2018;129:227-36.

[37] Tarleton RL. *Trypanosoma cruzi* and Chagas Disease: Cause and Effect. In: Tyler KM, Miles MA, editors. American Trypanosomiasis. Boston, MA: Springer US; 2003. p. 107-15.

[38] Bustamante JM, Tarleton RL. Methodological advances in drug discovery for Chagas disease. Expert Opin Drug Discov. 2011;6:653-61.

[39] Pinto MM, Sousa ME, Nascimento MS. Xanthone derivatives: new insights in biological activities. Curr Med Chem. 2005;12:2517-38.

[40] Sauer NN. Green Chemistry: Frontiers in Benign Chemical Syntheses and Processes Edited by Paul T. Anastas and Tracy C. Williamson (U. S. Environmental Protection Agency). Oxford University Press: New York, NY. 1999. 360 pp. $115.00. ISBN 0-19-850170-6. Journal of the American Chemical Society. 2000;122:5419-20.

[41] Wender PAH, S. L.; Wright, D. L. Towards the ideal synthesis. Chem Ind. 1997:765-9.

[42] Al-Massarani SM, El Gamal AA, Al-Musayeib NM, Mothana RA, Basudan OA, Al-Rehaily AJ, et al. Phytochemical, antimicrobial and antiprotozoal evaluation of Garcinia mangostana pericarp and alpha-mangostin, its major xanthone derivative. Molecules. 2013;18:10599-608.

[43] Abe F, Nagafuji S, Okabe H, Akahane H, Estrada M, ntilde, et al. Trypanocidal Constituents in Plants 3.Leaves of *Garcinia intermedia* and heartwood of *Calophyllum brasiliense*. Biological and Pharmaceutical Bulletin. 2004;27:141-3.

[44] Abe F, Nagafuji S, Okabe H, Higo H, Akahane H. Trypanocidal constituents in plants 2.xanthones from the stem bark of Garcinia subelliptica. Biol Pharm Bull. 2003;26:1730-3.

[45] Kelly JX, Winter R, Peyton DH, Hinrichs DJ, Riscoe M. Optimization of xanthones for antimalarial activity: the 3,6-bis-omega-diethylaminoalkoxyxanthone series. Antimicrob Agents Chemother. 2002;46:144-50.

[46] Fotie J, Nkengfack AE, Rukunga G, Tolo F, Peter MG, Heydenreich M, et al. *In-vivo* antimalarial activity of some oxygenated xanthones. Annals of Tropical Medicine & Parasitology. 2003;97:683-8.

[47] Tjahjani S. Antimalarial activity of Garcinia mangostana L rind and its synergistic effect with artemisinin in vitro. BMC Complement Altern Med. 2017;17:131.

[48] Zingales B, Miles MA, Moraes CB, Luquetti A, Guhl F, Schijman AG, et al. Drug discovery for Chagas disease should consider *Trypanosoma cruzi* strain diversity. Memorias do Instituto Oswaldo Cruz. 2014;109:828-33.

[49] Chatelain E, Konar N. Translational challenges of animal models in Chagas disease drug development: a review. Drug design, development and therapy. 2015;9:4807-23.

[50] Romanha AJ, Castro SLd, Soeiro MdNC, Lannes-Vieira J, Ribeiro I, Talvani A, et al. In vitro and in vivo experimental models for drug screening and development for Chagas disease. J Memórias do Instituto Oswaldo Cruz. 2010;105:233-8.

[51] Zingales B, Pereira ME, Oliveira RP, Almeida KA, Umezawa ES, Souto RP, et al. *Trypanosoma cruzi* genome project: biological characteristics and molecular typing of clone CL Brener. Acta Trop. 1997;68:159-73.

[52] Rossi MA, Mengel JO. Patogênese da miocardite chagásica crônica: o papel de fatores autoimunes e microvasculares. J Revista do Instituto de Medicina Tropical de São Paulo. 1992;34:593-9.

[53] Gutierrez FR, Mineo TW, Pavanelli WR, Guedes PM, Silva JS. The effects of nitric oxide on the immune system during *Trypanosoma cruzi* infection. J Memórias do Instituto Oswaldo Cruz. 2009;104:236-45.

[54] Afonina IS, Zhong Z, Karin M, Beyaert R. Limiting inflammation the negative regulation of NF-κB and the NLRP3 inflammasome. Nature Immunology. 2017;18:861.

[55] Ang E, Liu Q, Qi M, Liu HG, Yang X, Chen H, et al. Mangiferin attenuates osteoclastogenesis, bone resorption, and RANKL-induced activation of NF-kappaB and ERK. J Cell Biochem. 2011;112:89-97.

[56] Arthur JS, Ley SC. Mitogen-activated protein kinases in innate immunity. Nat Rev Immunol. 2013;13:679-92.

[57] Bistrian B. Systemic response to inflammation. Nutr Rev. 2007;65:S170-2.

[58] Callejas-Hernández F, Rastrojo A, Poveda C, Gironès N, Fresno M. Genomic assemblies of newly sequenced *Trypanosoma cruzi* strains reveal new genomic expansion and greater complexity. Scientific reports. 2018;8:14631-.

[59] Brener Z, Chiari E. Susceptibility of different strains of *Trypanosoma cruzi* to various chemotherapeutic agents. Rev Inst Med Trop Sao Paulo. 1967;9:197-207.

[60] Brener Z, Costa CA, Chiari C. Differences in the susceptibility of Trypanosoma cruzi strains to active chemotherapeutic agents. Rev Inst Med Trop Sao Paulo. 1976;18:450-5.

[61] Esper L, Talvani A, Pimentel P, Teixeira MM, Machado FS. Molecular mechanisms of myocarditis caused by *Trypanosoma cruzi*. 2015;28:246-52.

[62] de Paula Costa G, Silva RR, Pedrosa MC, Pinho V, de Lima WG, Teixeira MM, et al. Enalapril prevents cardiac immune-mediated damage and exerts anti-*Trypanosoma cruzi* activity during acute phase of experimental Chagas disease. Parasite Immunol. 2010;32:202-8.

[63] Leite ALJ, Paula Costa G, Lopes LR, Reis Mota LWD, Vieira PMA, Talvani A. The immunomodulatory effects of the Enalapril in combination with Benznidazole during acute and chronic phases of the experimental infection with *Trypanosoma cruzi*. Acta Trop. 2017;174:136-45.

[64] Guedes PM, Veloso VM, Talvani A, Diniz LF, Caldas IS, Do-Valle-Matta MA, et al. Increased type 1 chemokine expression in experimental Chagas disease correlates with cardiac pathology in beagle dogs. Vet Immunol Immunopathol. 2010;138:106-13.

[65] Marino Ana Paula MP, da Silva A, dos Santos P, Pinto Luzia Maria de O, Gazzinelli Ricardo T, Teixeira Mauro M, et al. Regulated on activation, normal T cell expressed and secreted (RANTES) antagonist (Met-RANTES) controls the early phase of *Trypanosoma cruzi* elicited myocarditis. Circulation. 2004;110:1443-9.

[66] Penas FN, Cevey ÁC, Siffo S, Mirkin GA, Goren NB. Hepatic injury associated with *Trypanosoma cruzi* infection is attenuated by treatment with 15-deoxy-Δ12,14 prostaglandin J2. Experimental Parasitology. 2016;170:100-8.

[67] Novaes RD, Santos EC, Cupertino MC, Bastos DSS, Oliveira JM, Carvalho TV, et al. *Trypanosoma cruzi* infection and benznidazole therapy independently stimulate oxidative status and structural pathological remodeling of the liver tissue in mice. Parasitology Research. 2015;114:2873-81.

Legend of figures

Figure 1. Synthesis of xanthenodiones 1-9 catalyzed by $ZrOCl_2 \cdot 8H_2O$. The compounds were obtained from the reaction of 1,3-diketones and aldehydes. Reaction conditions: 1,3-diketone (2.00 mmol), aldehyde (1.00 mmol), $ZrOCl_2 \cdot 8H_2O$ (2 mol%), 85°C.

Figure 2. Structures of tetraketones 10-12.

Figure 3. The effects of xanthenodiones inhibitors on *T. cruzi* amastigotes after 72 h of treatment. (A) Vero cell cultures were infected with Tdtomato-expressing trypomastigotes of CL strains (10:1 ratio parasites:cells). (B) Dose-response curve showing the inhibitory effect of **10**, **11** and **9** on *T. cruzi* amastigotes CLtdTomato strain on 3st day post-infection. Results are representative of three independent experiments with tree replicates.

Figure 4. Parasitemia and survival of Swiss mice infected with *T. cruzi* and treated with 9 and/or Bz. Mice were infected with *T. cruzi* (Y and CL strain 5×10^3 parasites/animal) and treated orally with 50 mg/kg of **9** for 10 consecutive days, as well as, another group of mice received 100mg/kg of Bz and/or only CMC (control group). (a) Parasitemia levels; (b) survival curves. The data are representative of the group average (10 mice per group) * means data statistically significant in relation to Bz-treated animals. Bz = benznidazole; NI = uninfected animals; NTI = uninfected mice treated with **9**; CMC (carboxymethylcellulose).

Figure 5. **Inflammatory mediators in the cardiac tissue during acute phase of *T. cruzi* infection**. (A) RankL, (B) CCL2, (C) IFN and (D) IL-10 were measured in by enzyme-linked immunosorbent assay in Swiss mice infected with Y and CL strains of *T. cruzi* (under treatment with **9** or Bz). In parallel, uninfected mice treated with **9** or untreated animals (control group) were also evaluated and all data shown as a mean of 10 animals ± SEM, and differences represented by $p<0.05$; Bz = benznidazole; NI = uninfected mice; NIT = uninfected mice treated with **9**; SEM = standard error of the mean.

Figure 6. **Quantification of the acute inflammatory process in the cardiac tissue of mice infected with *T. cruzi* Y and CL strains**. Analysis of inflammatory infiltration in cardiac tissue was performed after the mice treatment with **9** (50 mg/kg) or Bz (100 mg). Analysis of the inflammatory infiltration highlighting the polymorphonuclear (A) and mononuclear cells (B) Photomicrography of histological sections was performed on the cardiac tissue (C). Octagonal field diagram was organized in domains representing tissue cellularity as follows: (-) minimal cellularity / (+ -) mild, (+ +) moderate or (+ + +) intense / inflammatory infiltrate (D). (*) $p<0.05$ compared to the uninfected (NI) and uninfected/treated (NI**+9**)

control group; (#) p<0.05 compared to the animals treated with Bz and (&) p<0.05 compared to the animals treated with **9**. Bz = benznidazole; NI = uninfected mice; NIT = uninfected mice treated with **9.**

Figure 7. Illustrative panel of the trials carried out in this work Figure 7. Illustrative panel of the trials carried out in this work. (A) The first step was to test twelve xanthenodiones against CLtdTomado *T. cruzi* amastigotes. Irradiated Vero cell was platted ($2{,}5x10^4$/well) and infected by *T. cruzi* (10:1 ratio parasite/cell) and 72 h later the fluorescence was read as a measure of the growth (IC50 calculated). In parallel, the compounds toxicity was measured by AlamarBlue® reagent in Vero cells and CC50 was calculated. We obtained the SI through CC50/IC50 ratio and selected the best xanthenodione, named compound **9**, in the *in vitro* step, (B) Moving to the *in vivo* step, we tested 5 different doses 800 to 50mg/kg (1:2) and the treatment route (oral and intraperitoneal) and we assessment the parasitemia and survival levels in mice (n=5). (C) Then, we infected Swiss mice female by Y or CL *T. cruzi* strain and treated the animals by gavage, only, for 10 consecutive days(n=10) and, again, evaluated the parasitemia and survival levels. After the treatment period, animals were euthanized, and half section of heart used for histology. Another heart fragment was used for measurement of chemokines and cytokines by immunoassays (ELISA). We also analyzed the AST and ALT hepatic enzymes, urea and creatinine in the plasm to check the hepatic/renal compound toxicity.

Highlights

(i) The Xanthenediones and Tetraketones presented antitrypanosomal activity against ClTdtomato amastigotes *in vitro.*

(ii) In the mice infected with the Y strain of *T. cruzi*, the compound **9** reduced the parasitemia (40%) and prevented the mortality.

(iii) The compound **9** reduced the inflammatory cardiac infiltration in mice infected with Y and CL strains of *T. cruzi*.

(iv) The compound **9** increased the IL-10 in those animals infected with the CL strain of *T. cruzi* with no hepatic and renal toxicity.

Table 1. Vero cells toxicity, trypanocidal activity and xanthenodiones selectivity index

Compound	Vero cells	Amastigotes CL TdTomato	SI
	CC_{50}(µM)/SD	IC_{50}(µM)/SD	
1	>100	Inactive	ND
2	>100	Inactive	ND
3	>100	Inactive	ND
4	2.66	Inactive	ND
5	29.69	Inactive	ND
6	>100	Inactive	ND
7	27.8	Inactive	ND
8	43.58	Inactive	ND
9	>100	30.65 ± 1.0	3.2*
10	>100	14.11 = 1.9	7.2*
11	81.47	26.43 ± 2.3	3.0*
12	>100	Inactive	ND
Bz	>100	3.2 = 1.3	31.2

SD = Standard Error. (*) $p<0.05$ compared to benznidazol group. CC50 = 50 % Cytotoxicity concentrations. IC50 = 50% Inhibitory concentration. SI = Selective Index

Table 2. Ratio of inflammatory mediators/IL-10 in mice infected with Y and CL strains of *T. cruzi* under different treatments.

Groups	IFN/IL-10	CCL2/IL-10	RANK/IL-10
Y+Bz	0,08	0,39	0,24
Y+9	0,10	0,92	0,32
Y	0,09	0,87	0,32
CL+Bz	0,10	0,47	0,30
CL+9	0,12	0,86	0,39
CL	0,11	0,72	0,33

Table 3. Biochemical analysis (mean ± SD values) performed in infected mice after 14 (Y strain) and 18 (CL strain) days post *T. cruzi* infection

T. cruzi	Treatment	AST	ALT	Creatine	Urea
Y	Bz	132.9±25.5	98.44±31.0	0.34±0,2	41.59±7.5
	9	406.8±40.2*[#]	213,7±17.6*	0,43±0.1	36.5±14.8
	None	344±61.5*[#&]	213.8±53.3*	0.33±0.1	49.52±27.1
CL	Bz	163.6±16.6	90.18±28.8	0.31±0.1	51.57±5.6
	9	174,4±26.3	140,8±40.9	0.44±0,2	38.83±9.8
	None	125.6±29.4	156.8±29.4[#]	0.35±0.3	35.83±20.4
Uninfected	Bz	-	-	-	-
	9	161,5±22.6	103,9±24.0	0,29±0.2	58,11±9.6
	None	163,4±24.4	110,6±36.5	0,32±0.2	61,98±6.3

SD = Standard deviation. AST = aspartate amino transferase. ALT = alanine aminotransferase. (*) $p < 0.05$ compared to the uninfected (NI) and uninfected/treated (NI+9) control group. (#) $p < 0.05$ compared to the group treated with Bz (benznidazol). (&) $p < 0.05$ compared to the group treated with **9**

In vitro assays

Xanthenediones & Tetraketones

Amastigote forms CLTdTomato

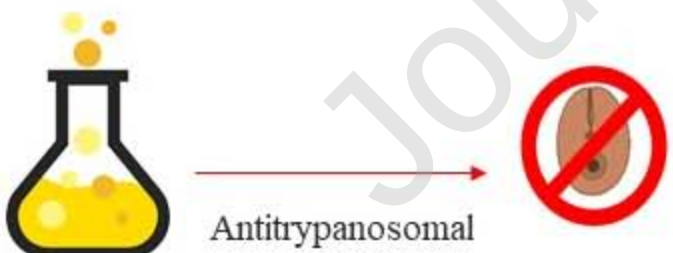

In vivo assays

Y strain and CL strains of *T. cruzi*

Euthanasia

10 days of treatment with the compound **9**

40% less parasites in the blood observed with the Y strain (*T. cruzi*) infection.

Cardiac tissue (histology)

Inflammatory infiltration

Immunological assays

IL-10 in infected mice (CL strain)

Biochemistry assays

No hepatic and renal toxicity